Defence Science Journal, Vol. 74, No. 2, March 2024, pp. 278-287, DOI : 10.14429/dsj.74.18685

Evaluation of Boron Combustion for Ducted Rocket Applications Using Condensed Product Analysis

Syed Alay Hashim[#,*], Srinibas Karmakar[$], Arnab Roy[$] and Muazu Abubakar[#]

[#]*Department of Aerospace Engineering, Alliance University, Bangalore - 562 106, India*
[$]*Department of Aerospace Engineering, Indian Institute of Technology, Kharagpur - 721 302, India*
[#]*Department of Mechanical Engineering, Bayero University Kano, PMB 3311, Nigeria*
[*]*E-mail: syed.hashim@alliance.edu.in*

ABSTRACT

Boron, a metalloid, produces high energy upon combustion. It is recommended as an ingredient for fuel or propellant in rocket propulsion, despite the challenge of extracting its full thermal energy. So far no one has claimed the complete energy conversion of boron upon combustion. On the other hand, the current propulsion system of the Meteor missile uses boron-loaded propellant. The boron-loaded propellant provides an approximately three-fold increase in specific impulse compared to conventional propellants. The present study focuses on boron-HTPB-based solid fuels impregnated with early ignited particles as additives, aiming to assess the combustion performance of boron particles. These additives are magnesium (Mg), titanium (Ti), and activated charcoal (C), and their effects are evaluated based on the residual active boron content in the condensed combustion products (burned residues). An economical tool commonly called stagnation flow or Opposed Flow Burner (OFB) is used to deflagrate the fuel sample by means of pressurized oxygen gas. The condensed combustion products are examined using a Field Emission Scanning Electron Microscope (FESEM), X-ray Diffraction (XRD), Thermo Gravimetric Analysis (TGA), and Differential Thermal Analysis (DTA). Among the fuel combinations investigated here, magnesium has been found to be a good burning enhancer of boron, leaving the lowest active boron content (30 %) in the burned-out residue. The current research aims to develop an efficient boron-containing solid fuel for hybrid propellant ducted rocket engine applications.

Keywords: Boron-based solid fuel; Additive loading; Thermal analysis; Residual products; Ducted rocket

NOMENCLATURE

Å	: Angstrom
G_{ox}	: Oxygen mass flux
K	: Shell
λ	: Wavelength
DTA	: Differential Thermal Analysis
FESEM	: Field Emission Scanning Electron Microscope
FPS	: Frame Per Second
HPDR	: Hybrid Propellant Ducted Rocket
HTPB	: Hydroxyl-Terminated Polybutadiene
IPDI	: Isophorone Diisocyanate
OFB	: Opposed Flow Burner
SFDR	: Solid Fuel Ducted Rocket
SFRJ	: Solid Fuel Ramjet
TGA	: Thermogravimetric Analysis
XRD	: X-ray Diffraction

1. INTRODUCTION

Boron, a metalloid, has long been attractive for Solid Fuel Ramjet (SFRJ) or Solid Fuel Ducted Rocket (SFDR) engines. Theoretically, boron produces a high combustion temperature and subsequent high energy, approximately 137 kJ/cm^3 and 58.7 kJ/g respectively on both volumetric and gravimetric basis[1-2]. However, it is difficult to achieve due to the formation of boron oxide (B_2O_3) coating on its surface, which delays the ignition/combustion process[3-6]. In this section, boron is highlighted first to reveal boron's ignition and combustion phenomena, followed by its application in propulsive devices.

Boron ignition and combustion are complicated and have been studied for many years by several researchers. Extensive research on boron ignition began about five decades ago and continues today. It is very interesting to note that the pioneering study is still well recognised and is considered a milestone for researchers working on boron. From previous literature, it is observed that the boron ignition temperature varies over a wide range. Large boron particles (agglomerated form) ignite between 527-827 ^oC, boron particle suspended in gas ignites between 827-1427 ^oC, and a single boron particle ignites between 1577-1727 ^oC, respectively[1,7-8]. A single boron particle (35-45 µm) was experimentally examined in 1969 by Macek and Semple to gain a better understanding of boron combustion mechanisms[1]. They discovered that there are two steps involved in the combustion of boron particles. Further similar observations have been found by another researchers[9-11]. The boron oxide layer slowly peels off the

Received : 16 December 2022, Revised : 06 October 2023
Accepted : 07 December 2023, Online published : 26 March 2024

boron's surface in the first stage, and in the second stage, the boron's core is revealed and eventually ignites with a brilliant flame. When the temperature of the boron particle rises, boron oxide melts (at ~450 °C) and forms a liquid layer around the particle, although, due to continuous heat transfer, some portion of the liquid boron oxide rapidly converts into vapor. In these conditions, a sizable diffusive barrier forms between pure boron and the oxidant, preventing the initial step (first stage) of boron combustion. Since the diffusion rate is comparatively slower than the kinetic rate, this stage of boron combustion is diffusion-limited[1]. Above the boiling temperature of boron oxide, the liquid boron oxide layer is completely vaporized, and the core boron starts melting. In this situation, the diffusion of oxygen becomes easier. Hence, it is considered that boron combustion is completely dependent on the local temperature and the amount of available oxygen[1,12].

In another experiment, Macek and Sample investigated the effect of oxidizer and pressure at 1727 °C using crystalline boron (75 µm) particles[13]. In this investigation, laser ignition has been implemented. They observed that when the pressure is increased from 1 to 35 atm, the burning time reduces from 45 ms to about 20 ms in air and oxygen/argon environments respectively. Further, the burning time is reduced to 6.5 ms in an oxygen environment. The basic concept behind the boron ignition and combustion mechanism has been demonstrated in Fig. 1. Yeh and Kuo conducted various experiments on both amorphous (2-3 µm) and crystalline (3 µm) boron particles using a flat flame burner[12]. In their single-particle analysis, they also found that boron burns in two stages. A theoretical model has been developed where the product of pressure (P) and particle diameter (D) expresses the nature of boron combustion (2nd stage). When PD >>75 atm-µm, diffusion of oxygen is dominated, PD << 75 atm-µm chemical kinetics is dominated, and PD ~ 75 atm-µm diffusions and kinetics both played their role in the 2nd stage combustion[12]. Li and Williams studied the combustion of a single boron particle where the particle is ejected into the hot gases of a flat flame burner[14]. T

hey observed three different plume colours: bright yellow, white, and green. Bright yellow signifies ignition, and a white glow denotes boron combustion where the green colour is identified as the intermediate species BO_2. BO_2 is readily identified during both ignition and combustion. Yetter, *et al.* developed a kinetic model of homogeneous gas-phase chemistry for B/O/H/C systems for the temperature range of 1527-2727 °C[15]. They included 19 chemical species with a total of 58 forward and reverse elementary reactions. It is observed that the initial stable suboxides/sub-oxyhydrides are first reduced to BO; further, they are oxidized to BO_2, and ultimately BO_2 is reduced into HBO_2 or B_2O_3. The formation of HBO_2/B_2O_3 in the product depends on the amount of water vapor contained in the reaction ($HBO_2 + HBO_2 \leftrightarrow B_2O_3 + H_2O$).

There is always a search for alternative technologies to accommodate larger payloads in the form of warheads and satellites in volume-limited systems like rockets and missiles. These propulsive devices need to be implemented with energetic fuel/propellant so that they can provide high speed and endurance while carrying a heavy payload. In this context, hydrocarbon fuels such as HTPB have been impregnated with metal fuel to enhance their energetic potential. From previous investigations, it seems that significant improvement in boron ignition and combustion has not been achieved yet. Indeed, this indicates a need for innovative and novel research strategies so that boron can be made a platform as a primary choice in rockets and ramjet variants. To overcome the difficulties associated with boron, various early ignited metal particles (or additives) such as titanium, magnesium, and iron have been tested with boron particles[4,6,16-17]. In this context, boron is tried with other propulsive devices such as Solid Fuel Ramjets (SFRJs) or Solid Fuel Ducted Rockets (SFDRs) to maximize the use of all its energy. It is typically advised to test the condensed combustion products on a lab-scale model before going on to a real rocket system to assess the burn performance in both cases: additive-loaded fuel and design-level alterations[4,18-20].

Among the ramjet variants, the solid fuel ducted rocket (SFDR) configuration is one in which the rocket motor is combined with the ramjet engine. SFDR does not require any external device to start from static conditions because this work is done by the integral rocket. Therefore, SFDR starts with zero forward speed. It generates a higher specific impulse than rocket motors and has a better specific thrust than ramjet variants[21-23]. In SFDR, the oxidizer to fuel ratio is kept low compared to conventional propellant so that, on combustion, it produces fuel-rich gases in the primary combustion chamber. The fuel-rich hot gases coming from the rocket motor (primary combustor) are further burned in the secondary combustion chamber with the help of bypass air (available from the atmosphere)[24].

In recent times, hybrid propellant-based ducted rockets have also been investigated, where the primary combustor is equipped with a hybrid propellant rocket motor[23]. Since nano-size fuel particles are involved in the current study and the nanoparticles are not readily available in bulk, a low-cost rapid

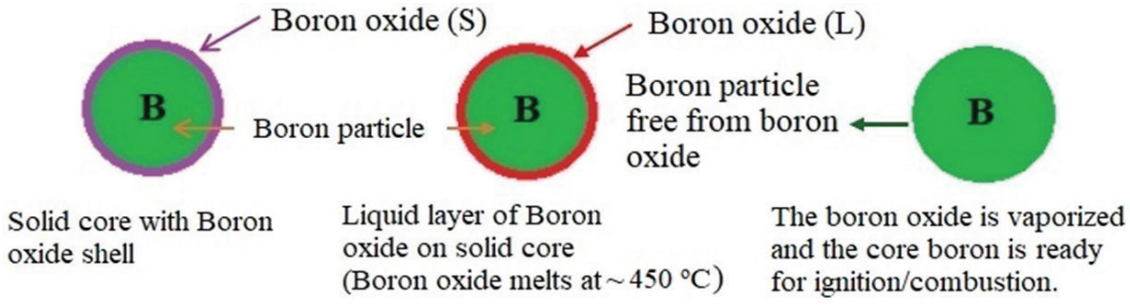

Figure 1. Physical stages involved in boron ignition and combustion.

screening instrument called an opposed flow burner (OFB) is used to make the research economical. Although OFB cannot be compared directly with a lab-scale rocket motor, which is used to evaluate the fuel or propellant performance in the primary stage. Since the 1950s, the opposed flow burner concept has been available in the literature and has been found in many studies evaluating fuel performance[25-27]. Therefore, OFB is considered as an affordable and rapid evaluating tool for the evaluation of solid fuel.

The current study is concerned with fuel component characterisation, processing of boron-loaded solid fuels, and combustion efficiency via post-combustion analysis. The fuel particles are processed into pellet shapes with the help of a polymeric binder, Hydroxyl-Terminated Polybutadiene (HTPB). To improve boron's ignition and combustion, magnesium (Mg), titanium (Ti), and activated charcoal (C) particles are impregnated with HTPB. An Opposed Flow Burner (OFB) with a more rigorous extension is used to investigate the combustion performance of boron-based metalized solid fuels. In a nutshell, burning performance analysis has been carried out at the microscopic level on the condensed combustion product of solid fuels. The aim of the study is to propose a boron-based solid fuel combination for use as an energetic fuel/propellant in a Hybrid Propellant Ducted Rocket (HPDR) engine.

2. METHODOLOGY

2.1 Materials

Fuel particles (boron, magnesium, titanium, and activated charcoal), curing agent Isophorone Diisocyanate (IPDI), and binder HTPB (R45) were obtained from various sources. Table 1 displays the details of the ingredients.

Table 1. Ingredient specifications, the data mentioned here was provided by the suppliers

Ingredient	Particle size	Purity (%)	Stock/ Product no.	Source
B	≤1µm	≥95	15580	Sigma Aldrich
Mg	<12 nm	99.9	NS6130-01-169	Nanoshel
Ti	<70 nm	99.9	NS6130-0-146	Nanoshel
C	<40 nm	95	NS6130-01-117	Nanoshel
IPDI	-	>97.5	L13759	Alfa Aesar
HTPB	-	-	Defence standard	Anabond Ltd., India

2.2 Sample Preparation

Four different polymeric solid fuels based on nanosized boron particles are the subject of the current investigation. The first fuel sample (B-HTPB) was processed with 10 % fuel (B), 81 % binder/fuel (HTPB), and 9 % curing agent (IPDI). In the other three samples, the boron content was reduced to 8 %, and the remaining 2 % by weight was loaded with magnesium (BM-HTPB), titanium (BT-HTPB), and activated charcoal (BC-HTPB). In every sample, the percentages of HTPB and IPDI were held constant. The distribution of fuel ingredients in the solid fuel sample is shown in Table 2.

Table 2. Distribution of fuel ingredients

Fuel sample	B (wt. %)	Mg (wt. %)	Ti (wt. %)	C (wt. %)	HTPB+IPDI (wt. %)
B-HTPB	10	–	–	–	90
BM-HTPB	8	2	–	–	90
BT-HTPB	8	–	2	–	90
BC-HTPB	8	–	–	2	90

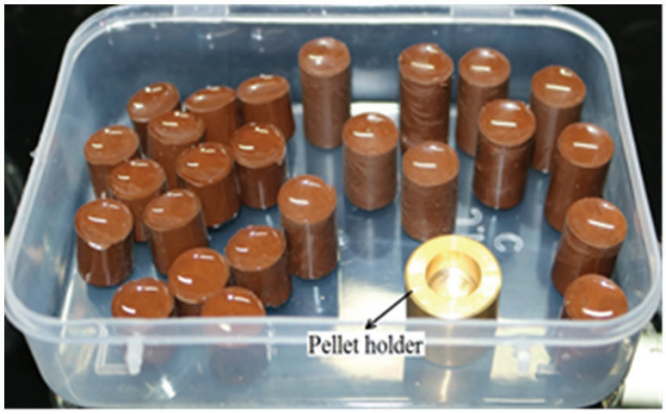

Figure 2. Boron-based solid fuel pellets.

The pure HTPB (binder) was used to begin the process of preparing the fuel sample. HTPB was first weighted in a clean beaker, followed by the curing agent IPDI, which was added and well mixed by hand for 20 min. To obtain the desired pellet shape, the HTPB-IPDI combination (semi-solid) was transferred into plastic dies with an internal diameter of 12.6 mm. The dies were then placed in a vacuum oven, which removed any air bubbles that had been caught in the mixture during the mixing of the components as well as dried the mixture. To break up air bubbles, degassing is always advised when handling solid fuels or propellants. In the current investigation, the mixture was baked for 5 days at 60 °C before being stored at room temperature (30 °C) for 25 days. On the basis of earlier findings, it was noticed that pellets (Fig. 2) were fully solidified after 30 days[19]. A similar procedure was followed in the preparation of remaining samples containing fuel particles. The fuel particles were introduced one by one to the HTPB-IPDI mixture and stirred for 20 min. In order to prevent local oxidation, the particles were the major focus; hence, when measuring and mixing the particles with HTPB, a nitrogen field glove bag was employed. Since nanoparticles are highly prone to oxidation, they use local air to generate oxides on their surfaces, which slows down the burning performance of the particles during combustion.

2.3 Material Characterization

A few material characterization techniques were used to examine the fuel components and burned byproducts of B-HTPB, BM-HTBP, BT-HTBP, and BC-HTBP. Field emission scanning electron microscope, FESEM (model: JSM-7610F), and X-ray diffraction, XRD (X'Pert3 Powder, utilizing CuKα (λ = 1.5418 Å) radiation) were used to examine the morphology and composition/structure of the powered sample. To minimize

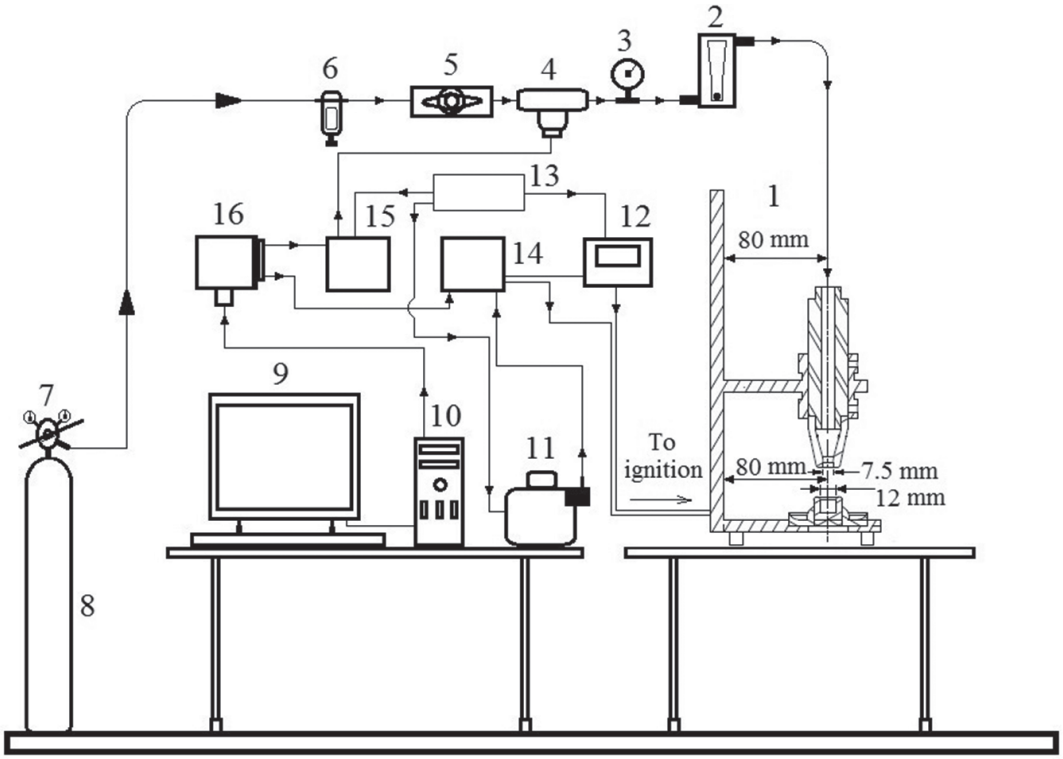

Figure 3. Schematic of opposed flow burner system: (1) OFB; (2) Rotameter; (3) Pressure gauge; (4) Solenoid valve; (5) Valve; (6) Humidifier/filter; (7) Regulator; (8) Oxygen cylinder; (9) PC monitor; (10) CPU; (11) Variac; (12) Amp. meter; (13) Supply board (AC); (14 and 15) Relay; (16) Data acquisition[19].

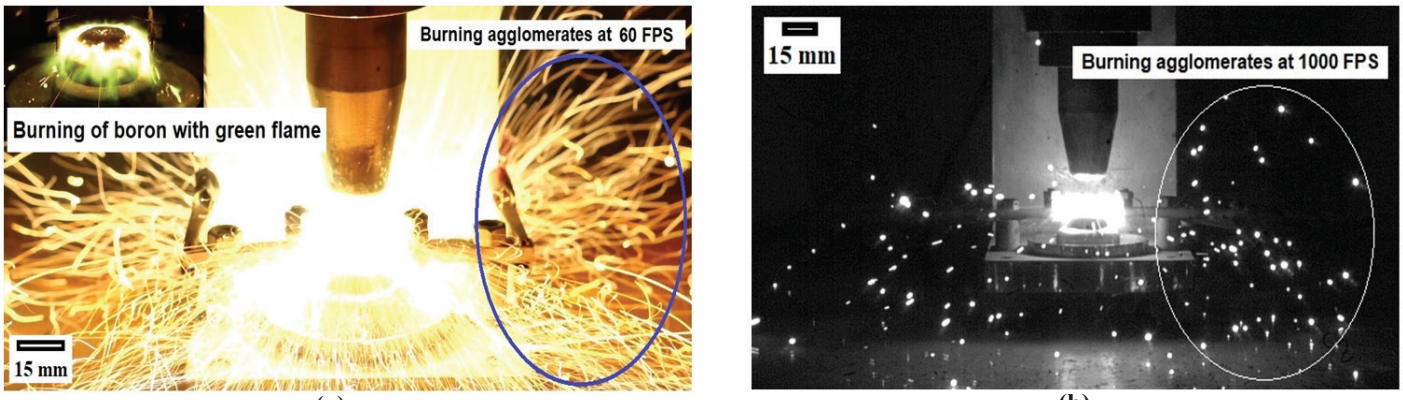

(a) **(b)**

Figure 4. Visualisation of burning agglomerates ejected out from the burning surface and burning of boron particles (a). FPS stands for frame per second of the camera; (a) Image by a DSLR camera (Nikon 1 V1); and (b) Image by a high-speed camera (Phantom V7.3).

the charge effects in the FESEM examination of the sample, a gold coating was applied using the ion sputtering technique. In the XRD, the angle 2θ ranged from 10° to 60°, while the scanning rate was fixed at 5°/min. The amount of active boron in the sample was determined with the help of Thermogravimetric Analysis (TGA) and Differential Thermal Analysis (DTA). The TGA/DTA system (Model: Pyris Diamond) was operated in an air environment, with the air supply set to 100 ml/min. In each sample analysis, the heating rate was kept constant at 10 °C/min.

2.4 Combustion Testing Tool

Opposing Flow Burner (OFB) was used to examine the combustion process in accordance with the detailed protocol covered in the prior work[19]. The essential components of the OFB are the nozzle (for oxygen supply), a pellet holder, and a stand. The OFB was associated with the ignition system and the oxygen supply line, and the complete configuration (Fig. 3) was controlled by a computer running LabVIEW software. The ignition wires (Fig. 3) were connected to a piece of tungsten wire that touched the surface of the solid fuel. When current flows to tungsten wire, the wire becomes red hot, and then the solid fuel surface ignites with the help of oxygen. The OFB was set at 30 kg/m^{2}s (oxygen mass flux, G_{ox}) to burn the samples, and all the fuel combinations were examined at the same settings and the system was run for 5 sec. The burned or condensed products are those particles that were ejected from the burning surface; they are called burning agglomerates (Fig. 4). These agglomerates move away from the burning surface like an asteroid and lose energy continuously. Finally, the

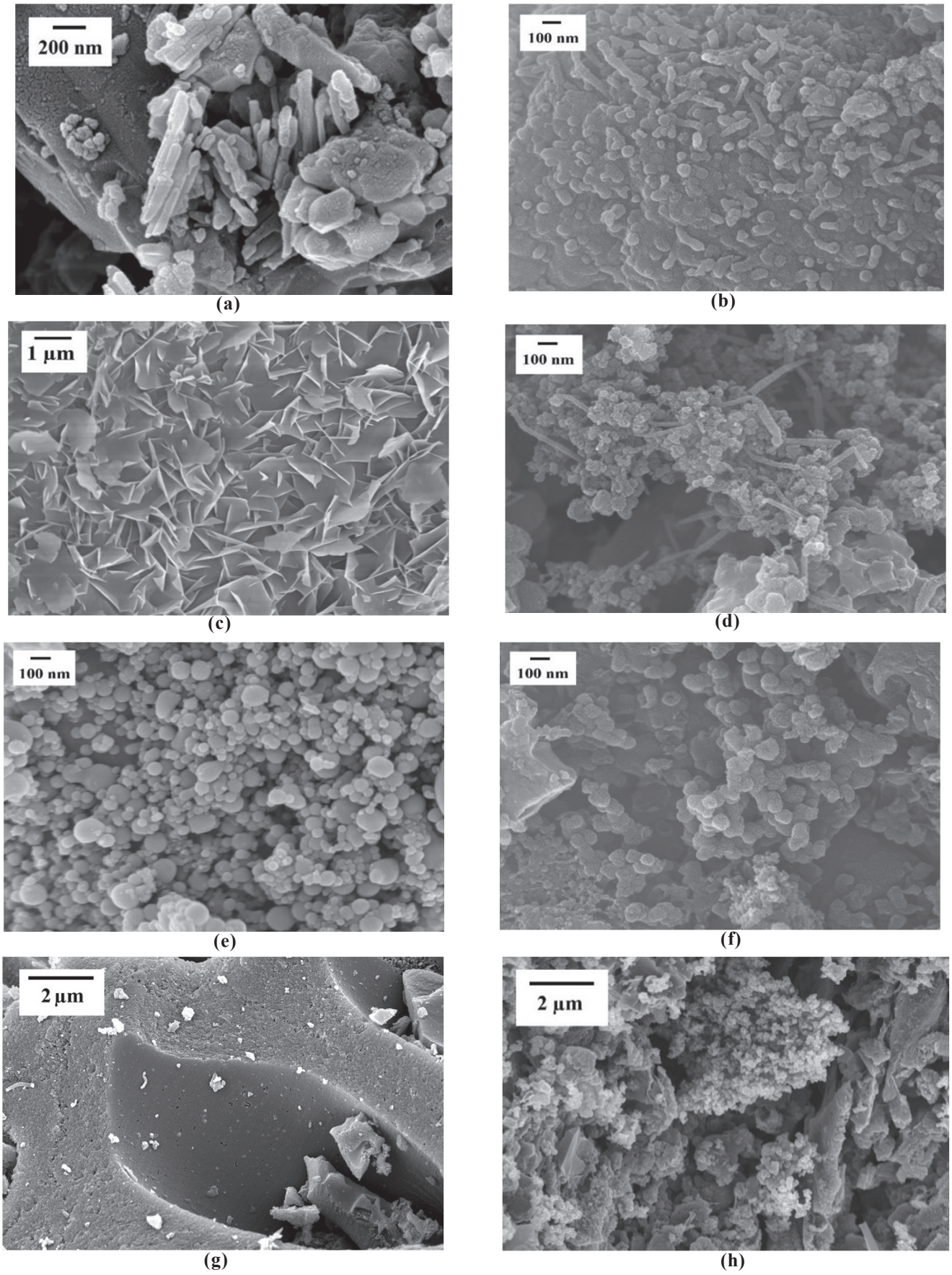

Figure 5. FESEM images of samples; (a) Pure B; (b) B-HTPB; (c) Pure Mg; (d) BM-HTPB; (e) Pure Ti; (f) BT-HTPB; (g) Pure C and (h) BC-HTPB.

burning agglomerates appear to be scalded materials dispersed close to the OFB system. These condensed products were carefully collected and sent for the material characterisation.

3. RESULTS AND DISCUSSION

3.1 FESEM Analysis

Figure 5 depicts the morphology of fuel particles and combustion products. Figure 5(a) shows a needle-like structure of B_2O_3 on the boron surface[4]. Figures 5(c), 5(e), and 5(g) show loosely bounded flake structures of magnesium, regular spherical shape of titanium, and porous charcoal particles[4,28]. Figure 5(d) (BM-HTPB) displays a mixture of spherical products of MgO produced by the oxidation of Mg and needle-like structures of B_2O_3 (Fig. 5(a) and 5(b)/B-HTPB)[4]. Cauliflower-like collections of TiO_2, H_3BO_3/B_2O_3, and TiB_2 are embedded in the matrix of the charred sample in Fig. 5(f) (BT-HTPB)[17,29]. Additionally, the burned byproduct of the sample made of charcoal contains B_2O_3 filaments (Fig. 5(h)) as well. It is not common to see burnt products in standardized sizes. In fact, these structures originated because of the solidification of melted elements from the burning surface that were subjected to temperature and pressure (or aerodynamics) loads caused by oxygen impingement.

Furthermore, flying agglomerate shapes released from the burning surface cannot be predicted if they are in the form of fine burning particles. The surface morphology of as-received charcoal powder exhibits fine pores. It is expected that when boron and charcoal particles were mixed while processing, tiny particles of both charcoal and boron were accommodated inside the charcoal pores (Fig. 5(g)). As a result, it is possible that, under burning conditions, charcoal pores play a significant role in improving the combustion process. On the other hand, the high oxygen diffusion in the voids of charcoal cannot be denied in terms of enhancing the combustion process on the burning surface of solid fuel. In this way, the total burning performance of boron is projected to improve the BC-HTPB sample. Because of the flaky structure of magnesium, it also enters the picture and suggests superior burning performance. It is possible to burn magnesium flakes quickly, which may boost the rate of boron combustion. In addition, the low melting point and high thermal conductivity of magnesium are likely to improve the burning of boron particles[25,30]. Magnesium burns as it melts; therefore, the thermal energy supplied by the magnesium particles aid boron in overcoming its ignition and combustion issues. Similarly, thermal energy is transferred to neighbouring boron particles at a high rate due to the higher thermal conductivity of magnesium. In the case of BT-HTPB, titanium ignites before melting, resulting in a quick energy increase for boron particles[31].

However, the morphological examination of titanium, which played a role in increasing combustion, revealed no significant form. Similar spherical structures can be seen in the BT-HTPB burnt product, which is boron oxide. Since the EDS examination on different parts of the material found no indication of titanium, the early ignition of additives due to particle shape and other features is expected to increase the burning performance of boron in solid fuels.

3.2 XRD Analysis

Figure 6 shows X-ray diffraction patterns of pure fuels (B, Mg, Ti, and C) and residual combustion products of B-HTPB, BM-HTPB, BT-HTPB, and BC-HTPB. The diffractograms are used to highlight the phase of the fuels and to identify the products formed during combustion. Figure 6(a) shows the crystal planes of boron (B: ICDD # PDF 00-011-0617), magnesium (Mg: ICDD # PDF 00-035-0821) and titanium (Ti: ICDD # PDF 01-072-4624). Minor peaks of boron oxide (at $2\theta = 14.7°, 28.4°$), magnesium oxide (at $2\theta = 36.9°$), and titanium oxide (at $2\theta = 36°$, 42.5, and 52°) have been identified in their respective XRD plots[4,16]. The XRD pattern of charcoal reveals

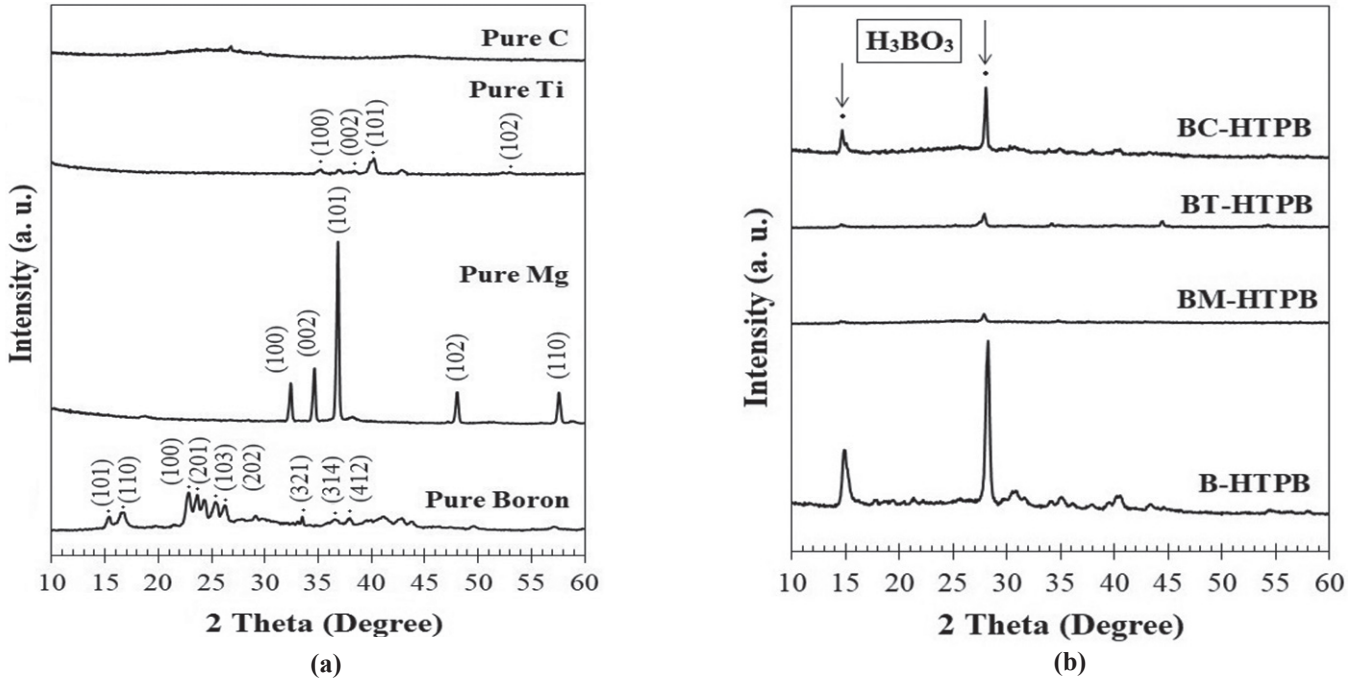

Figure 6. XRD diffractograms: (a) Pure; and (b) Burned residue.

a hump-like structure at the 2θ range of 23.4 - 34.6°, which is a typical peak range of amorphous carbon[32].

Similarly, the XRD pattern of burned B-HTPB (Fig. 6(b) exhibits prominent boric acid (H_3BO_3) peaks at 14.5° and 28°, with minor peaks at 29.54°, 30.56°, 31.44°, 34.90°, and 39.91°, 40.28°, and 44.8° (H_3BO_3: ICDD PDF#00-030-0620)[4,5]. The burned products of BM-HTPB, BT-HTPB, and BC-HTPB show a few peaks of H_3BO_3 at around 2θ = 14.5° and 28.2° with similar plane values as B-HTPB. However, among these additive-based samples only BC-HTPB exhibits sharp boric acid peaks. Boric acid is formed because of the reaction of boron oxide with water vapor/moisture during combustion. Consequently, dissimilarities in XRD patterns can be expected even though similar boron percentages are present in all additive-loaded samples. Since the condensed products are the flying burning agglomerates, their combustion does not create a typical scenario chemically among agglomerates. As a result, the sharpness of the peaks associated with H_3BO_3 varies. Furthermore, BT-HTPB has identified a few tiny peaks of Ti at 57.5°, TiO_2 at 48.1° and 54.4°, and TiB_2 at 34.16° and 44.5°. Simultaneously, condensed products of BM-HTPB, BT-HTPB, and BC-HTPB have minor peaks of boron carbine (B_4C) at 2θ = 34.8° and 37.7° [4].

3.3 Thermal Analysis

Figure 7 shows the curves for the differential thermal analysis (DTA) and thermogravimetric analysis (TGA) of pure boron and condensed products. The thermal study concentrated mostly on mass gain/loss and temperature-dependent reactions (exothermic or endothermic). The DTA curve of pure B

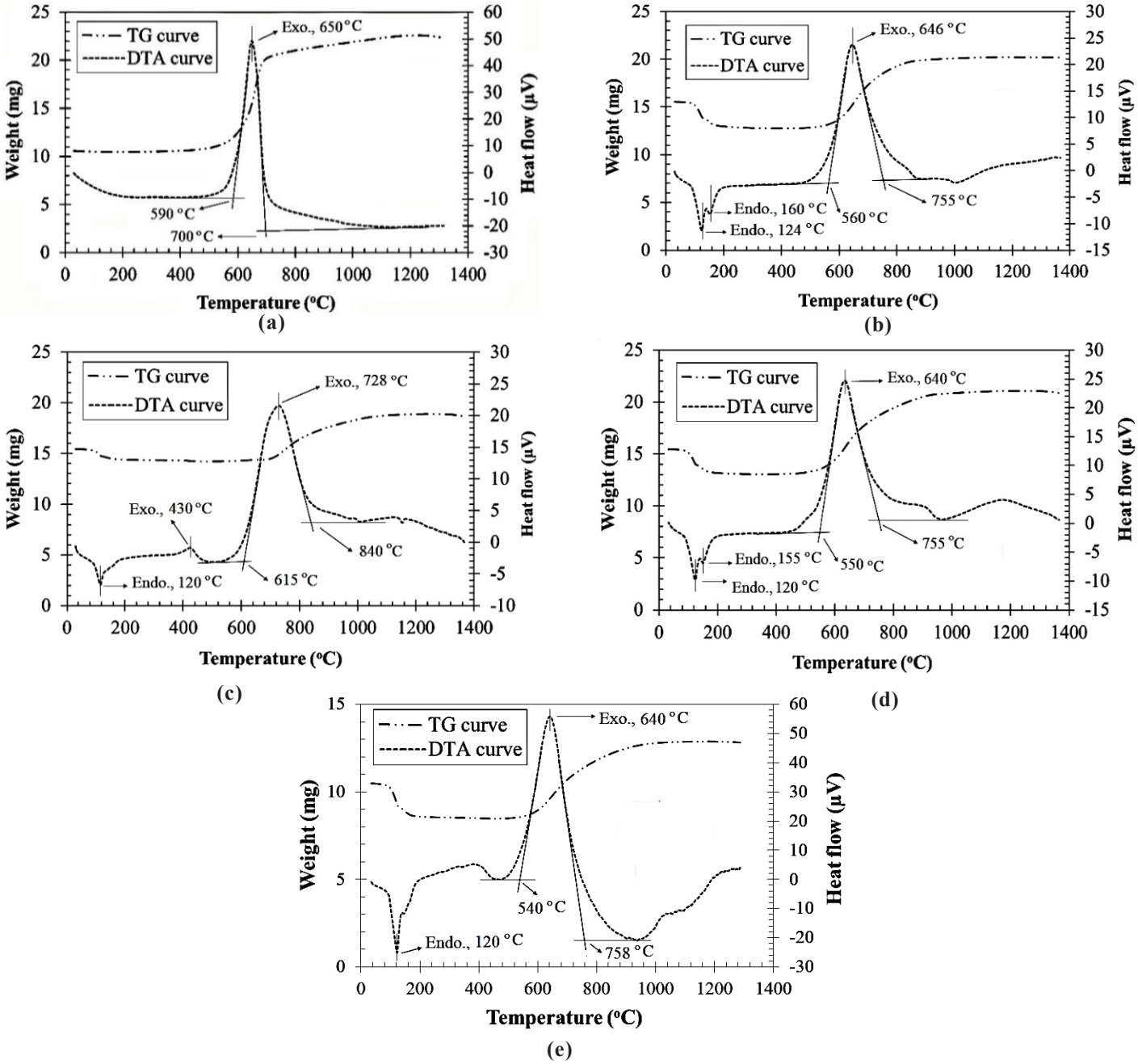

Figure 7. Thermal analysis of samples; (a) Pure boron; (b) B-HTPB; (c) BM-HTPB; (d) BT-HTPB and (e) BC-HTPB.

(Fig. 7(a)) shows a horizontal tangential line towards the onset temperature (~590 °C) of the boron particles. The range of onset temperature indicates the presence of native B_2O_3 (melting point 450 °C), which served as a protective coating on the boron surface. Eventually, the onset temperature shifts to the right. A sharp exothermic peak is found at ~650 °C due to the rapid oxidation of the boron particles, followed by the finishing temperature occurring at ~700 °C. As the temperature rises beyond ~590 °C, liquid B_2O_3 vaporizes, and eventually, core boron gets exposed to the oxidation reaction[19-20,33-34]. TG analysis found a large mass gain (~66 %) between 590-700 °C and showed a higher heat flow.

The DTA curve for burned B-HTPB shows two endothermic peaks (Fig. 7(b)); peak at 124 °C arises due to the hygroscopic sample (H_3BO_3), whereas the peak at 160 °C is due to the absorption of heat by the dehydrated boric acid (B_2O_3). The dehydrated sample (where mass loss is ~22 %) begins to react slowly with oxygen up to the onset temperature (560 °C)[20]. Above 560 °C, the evaporation process of liquid B_2O_3 rises; as a result, a sharp exothermic peak is attained at ~646 °C. Eventually, significant boron oxidation is observed between 560-755 °C (mass gain ~42 %). Similarly, an exothermic peak is observed at 430 °C in BM-HTPB due to the oxidation of exposed unburned Mg. The flaky Mg in the solid fuel enhances boron combustion in the OFB test and forms dense B_2O_3 in the condensed product. Consequently, the predominant temperatures are moved to the higher sides (Fig. 7(c)). Ultimately, only 20 % of the mass is gained between 615–840 °C. Figures 5(d) and 5(e) show DTA and TGA plots for BT-HTPB and BC-HTBP, where mass gains of ~38 % and ~33 % have been evaluated for BT-HTPB and BC-HTPB samples, respectively. The mass gain has been found between 540–760 °C.

In the present sample (BC-HTPB), there is a possibility of oxidation to the unburned carbon and the boron carbide (B_4C) formed during combustion[19-20]. The formation of boron carbide has been identified in the XRD analysis. In the comprehensive TG analysis between 30–1400 °C, the active boron is found to be 77 % in the pure boron sample. The residual active boron in the burned samples has also been estimated to be as follows: 50 % for B-HTPB, 30.3 % for BM-HTPB, 53 % for BT-HTPB, and 41.2 % for BC-HTPB, respectively. Among the four fuel combinations, condensed combustion products of magnesium and activated charcoal-based samples reveal the minimum residual boron content. Since higher thermal conductivity of magnesium energizes local fuel layers and the porous structure of activated charcoal disperses more oxygen. As a result, the combustion process is enhanced in the OFB analysis[25,30]. The visual identification of flame during combustion is analysed using images captured by a colour camera (Fig. 4(a)). An intense green emission from the flame has been identified on the burning surface of the boron-based solid fuels. The green emissions in the current study are intermediate species of boron that are formed during combustion. These species are BO and BO_2, and their wavelengths are between 400-580 nm[35-40]. Boron combustion is difficult, so visual observation is significant in two ways: (i) evaluating the burning performance of an opposed flow burner in the current study, and (ii) understanding the ignition and combustion properties of boron-based solid fuels. Therefore, visual identification in the case of boron-loaded fuels aids in the subsequent examination of the combustible product using material characterization techniques.

4. CONCLUSIONS

Boron-based solid fuels are processed with magnesium, titanium, and activated charcoal particles as a burning enhancer. These additives are only 2 % needed to maintain the maximum heat of combustion of the boron-loaded solid fuel combinations. An opposed flow burner (OFB) is used to evaluate the performance of the solid fuels. Among the four fuel combinations, the magnesium and charcoal-based samples performed well in terms of the residual active boron content in the combustible products, which is around 30 and 41 %, respectively.

The primary cause behind a high residual active boron content in the condensed products is ejection of the enormous volumes of burning agglomerates from the burning surface. These agglomerates transport the energy from the burning surface and release it away from the burning zone. Therefore, the subsequent layers underneath the solid fuel's burning surface receive significantly less thermal energy. As a result, the amount of energy needed to thoroughly burn fuel particles as they leave the burning surface is reduced. The mixing of early ignited particles (Mg, Ti, and C) in the present study enables boron to burn on the burning surface as well as contribute energy to burn agglomerates during ejection. It is expected that the reactivity of boron will improve with increased local pressure and temperature, which means that the percentage of residual active boron content in a rocket motor test can be further reduced with minor additive loadings.

REFERENCES

1. Macek, A. & Semple, J.M. Combustion of boron particles at atmospheric pressure. *Combust. Sci. Technol.,* 1966, **1**(3), 181–191. doi: 10.1080/00102206908952199.
2. Risha, G.A.; Evans, B.J.; Boyer, E. & Kuo, K.K. Metals, energetic additives, and special binders used in solid fuels for hybrid rockets, *Prog. Astronaut. Aeronaut.,* 2007, **218**, 413–456. doi: 10.2514/5.9781600866876.0413.0456
3. Yuasa, S. & Isoda, H. Ignition and combustion of small boron lumps in an oxygen stream. *Combust. Flame,* 1991, **86**, 216–222. doi: 10.1016/0010-2180(91)90101-g
4. Hashim, S.A.; Karmakar, S. & Roy, A. Effects of Ti and Mg particles on combustion characteristics of boron–HTPB-based solid fuels for hybrid gas generator in ducted rocket applications. *Acta Astronaut.,* 2019, **160**, 125–137. doi: 10.1016/j.actaastro.2019.04.002
5. Rosenband, V.; Natan, B. & Gany, A. Ignition of boron particles coated by a thin titanium film. *J. Propul. Power,* 1995, **11**(6), 1125–1131. doi: 10.2514/3.23950
6. Chintersingh, K.L.; Schoenitz, M. & Dreizin, E.L. Combustion of boron and boron–iron composite particles

in different oxidizers. *Combust. Flame,* 2018, **192**, 44–58.
doi: 10.1016/j.combustflame.2018.01.043

7. Shevchuk, V.G.; Zolotko, A.N. & Polishchuk, D.I. Ignition of packed boron particles. *Combust. Explos. Shock Waves,* 1975, **11**(2), 189–192.
doi: 10.1007 %2Fbf00756716
8. Zolotko, A.N.; Klyachko, L.A.; Kopeika, K.M.; Polishchuk, D.I. & Shevchuk, V.G. Critical ignition conditions for boron particles suspended in a gas. *Combust. Explos. Shock Waves,* 1977, **13**(1), 31–36.
doi: 10.1007/bf00756014
9. Ulas, U.; Kuo, K.K. & Gotzmer, C. Ignition and combustion of boron particles in fluorine-containing environments. *Combust. Flame,* 2001, **127**(1-2), 1935–1957.
doi: 10.1016/s0010-2180(01)00299-1
10. Ao, W.; Yang, W.; Wang, Y.; Zhou, J.; Liu, J. & Cen, K. Ignition and combustion of boron particles at one to ten standard atmospheres. *J. Propul. Power,* 2014, **30**(3), 760–764.
doi: 10.2514/1.b35054
11. Young, G.; Roberts, C.W. & Stoltz, C.A. Ignition and combustion enhancement of boron with polytetrafluoroethylene. *J. Propul. Power,* 2015, **31**(1), 386–392.
doi: 10.2514/1.b35390
12. Yeh, C.L. & Kuo, K.K. Ignition and combustion of boron particles. *Prog. Energ. Combust. Sci.,* 1996, **22**(6), 511–541.
doi: 10.1016/s0360-1285(96)00012-3
13. Macek, A. & Semple, J.M. Combustion of boron particles at elevated pressures. *13th Symp. (Int.) Combust.,* 1971, **13**(1), 859–868.
oi: 10.1016/s0082-0784(71)80087-5
14. Li, S.C.; Williams, F.A. & Takahashi, F. An investigation of combustion of boron suspensions. *22nd Symp. (Int.) Combust.,* 1988, **22**(1), 1951-1960.
doi: 10.1016/s0082-0784(89)80210-3
15. Yetter, R.A.; Rabitz, H.; Dryer, F.L.; Brown, R.C. & Kolb, C.E. Kinetics of high-temperature B/O/H/C chemistry. *Combust. Flame,* 1991, **83**(1-2), 43–62.
doi: 10.1016/0010-2180(91)90202-M
16. Liu, L.; Liu, P. & He, G. Ignition and combustion characteristics of compound of magnesium and boron. *J. Therm. Anal. Calorim.,* 2015, **121**(3), 1205–1212.
doi: 10.1007/s10973-015-4653-6
17. Sinthiya, M.AM.A.; Kumaresan, N.; Ramamurthi, K. & Sethuraman, K. Development of pure rutile TiO_2 and magneli titanium sub-oxide microstructures over titanium oxide seeded glass substrates using surfactant free hydrothermal process. *Bull. Mater. Sci.,* 2019, **42**(3), 1–8.
doi: 10.1007/s12034-019-1791-7
18. Hashim, S.A.; Karmakar, S. & Roy, A. Combustion characteristics of boron–HTPB-based solid fuels for hybrid gas generator in ducted rocket applications. *Combust. Sci. Technol.,* 2018, **191**(11), 1–19.
doi: 10.1080/00102202.2018.1544973
19. Hashim, S.A.; Islam, M.; Kangle, S.M.; Karmakar, S. & Roy, A. Performance evaluation of boron/hydroxyl-terminated polybutadiene-based solid fuels containing activated charcoal. *J. Space. Rock.,* 2021, **58**(2), 363–374.
doi: 10.2514/1.a34820
20. Hashim, S.A.; Karmakar, S. & Roy, A. Experimental observation and characterization of B–HTPB-based solid fuel with addition of iron particles for hybrid gas generator in ducted rocket applications. *Propel. Explos. Pyrotech.,* 2019, **44**, 1–13.
doi: 10.1002/prep.201900009
21. Davenas, A. Solid rocket propulsion technology. Pergamon Press, New York, 1992. 328-367 p.
doi:10.1016/c2009-0-14818-3
22. Gany, G. & Netzer, D.W. Fuel performance for the solid-fueled ramjet. *Int. J. Turbo Jet Engines,* 1985, **2**(2), 157–168.
doi: 10.1515/tjj.1985.2.2.157
23. Komornik, D. & Gany, A. Study of a hybrid gas generator for a ducted rocket. *Combust. Explos. Shock Waves,* 2017, **53**(3), 293–297.
doi: 10.1134/s0010508217030066
24. Obuchi, K.; Tanabe, M. & Kuwahara, T. Ignition characteristics of boron particles in the secondary combustor of ducted rockets-effects of magnalium particle addition. *46th AIAA Aerosp. Sci. Meet. Exhibit,* Reno, Nevada, 2008, 1–8.
doi: 10.2514/6.2008-943
25. Shark, S.C.; Zasck, C.R.; Pourpoint, T.L. & Son, S.F. Solid fuel regression rate and flame characteristics in an opposed flow burner. *J. Propul. Power,* 2014, **30**(1), 1675–1682.
doi: 10.2514/1.b35249
26. Young, G.; Risha, G.A., Miller, A.G.; Glass, R.A.; Connell, T.L. & Yetter, R.A. Combustion of alane-based solid fuels. *Int. J. Energetic Mater. Chem. Propuls.,* 2010, **9**(3), 249–266.
doi:10.1615/intjenergeticmaterialschemprop.v9.i3.50
27. Young, G.; Roberts, C. & Dunham, S. Combustion behavior of solid oxidizer/gaseous fuel diffusion flames. *J. Propuls. Power,* 2013, **29**(2), 362–370.
doi: 10.2514/1.b34568
28. Wei, J., Sun, H.; Zhang, D.; Gong, L.; Lin, J. & Wen, C. Influence of heat treatments on microstructure and mechanical properties of Ti–26Nb alloy elaborated in situ by laser additive manufacturing with Ti and Nb mixed powder. *Mater.,* 2019, **12**(1), 1–13.
doi:10.3390/ma12010061
29. Subramanian, T.C.S.R; Murthy, T.C. & Suri, A.K. Synthesis and consolidation of titanium diboride. *Int J Refract. Hard Met.,* 2007, **25**(4), 345–350.
doi: 10.1016/j.ijrmhm.2006.09.003
30. Sandall, E.; Kalman, J.; Quigley, J.N.; Munro, S. & Hedman, T.D.A. study of solid ramjet fuel containing boron–magnesium mixtures. *Propuls. Power Res.,* 2017, **6**(4), 243–252.
doi: 10.1016/j.jppr.2017.11.004

31. Abbud-Madrid, A.; Fiechtner, G.; Branch, M. & Daily, J. Ignition and combustion characteristics of pure bulk metals-normal-gravity test results. *32nd AIAA Aerosp. Sci. Meet. Exhibit,* Nevada, 1994. doi: 10.2514/6.1994-574
32. Shang, H.; Lu, Y.; Zhao, F.; Chao, C.; Zhang, B. & Zhang, H. Preparing high surface area porous carbon from biomass by carbonization in a molten salt medium. *RSC Adv.,* 2015, **5**(92), 75728–75734. doi: 10.1039/c5ra12406a
33. Jain, A. & Anthonysamy, S. Oxidation of boron carbide powder. *J. Therm. Anal. Calorim.,* 2015, **122**(2), 645-652.
34. Krauss, W.; Schanz, G. & Steiner. H. TG-rig tests (thermal balance) on the oxidation of B_4C. *Basic experiments, modelling and evaluation approach*, *Rep.* FZKA 6883, 2003.
35. Gaydon, A.G. The Spectroscopy of Flames. second ed., Halsted Press, New York, 1974. doi: 10.1007/978-94-009-5720-6
36. Weismiller, M.R.; Huba, Z.J.; Tuttle, S.G.; Epshteyn, A. & Fisher, B.T. Combustion characteristics of high energy Ti–Al–B nanopowders in a decane spray flame. *Combust. Flame,* 2017, **176**, 361–369. doi: 10.1016/j.combustflame.2016.10.025
37. Pearse, R.W.B. & Gaydon, A.G. The Identification of Molecular Spectra. fourth ed., Chapman and Hall, London, 1976. doi: 10.1007/978-94-009-5758-9
38. Liang, D.; Liu, J.; Zhou, Y. & Zhou, J. Ignition and combustion characteristics of amorphous boron and coated boron particles in oxygen jet. *Combust. Flame,* 2017, **185**, 292–300. doi: 10.1016/j.combustflame.2017.07.030
39. Robinson, J.W. Handbook of Spectroscopy. first ed., CRC Press, Cleveland, 1974.
40. Foelsche, R.; Burton, R. & Krier, H. Boron particle ignition and combustion at 30–150 atm. *Combust. Flame,* 1999, **117** (1–2), 32–58. doi: 10.1016/s0010-2180(98)00080-7

ACKNOWLEDGEMENT

This study has been supported by Alliance University, Bangalore, India and Indian Institute of Technology, Kharagpur, India. The authors are grateful for the resources provided by the institutions.

CONTRIBUTORS

Dr Syed Alay Hashim obtained his PhD from the Indian Institute of Technology, Kharagpur. He currently serves as an Associate Professor in the Department of Aerospace Engineering at Alliance University, Bangalore, Karnataka. His areas of interest inlclude: Boron combustion for hybrid fuel ducted rocket engines, nano-metallized-based fuels/propellants, and combustor for micro gas turbine engines.
His contribution to the present study includes: Planning, testing, analysis, and manuscript preparation.

Dr Srinibas Karmakar is working as an Associate Professor at IIT Kharagpur, West Bengal. His research areas include: Combustion of solid fuel, droplet and spray combustion, alternative aviation fuels, energetic particles, and development of green propellants etc.
He has reviewed, edited, and oversaw the research for the present work.

Dr Arnab Roy is working as a Professor at IIT Kharagpur, West Bengal. His research areas include: Computational fluid dynamics, low Reynolds no. aerodynamics, single and multiphase fluid dynamics, flapping wing aerodynamics, and aerospace propulsion etc.
He has edited, examined, and supervised the research for the present work.

Dr Muazu Abubakar is working as a Senior Lecturer at Bayero University Kano, Nigeria. His research areas include: Clay based-ceramics, ceramic membrane, cathodic protection, wastewater treatment, metals-alloys development, heat treatment, and metals extraction.
He has worked on thermal analysis of burnt products for the current study.